AIP | Applied Physics Letters

Intense green-yellow electroluminescence from Tb+-implanted silicon-rich silicon nitride/oxide light emitting devices

Y. Berencén, R. Wutzler, L. Rebohle, D. Hiller, J. M. Ramírez et al.

Citation: Appl. Phys. Lett. **103**, 111102 (2013); doi: 10.1063/1.4820836
View online: http://dx.doi.org/10.1063/1.4820836
View Table of Contents: http://apl.aip.org/resource/1/APPLAB/v103/i11
Published by the AIP Publishing LLC.

Intense green-yellow electroluminescence from Tb^+-implanted silicon-rich silicon nitride/oxide light emitting devices

Y. Berencén,[1,a)] R. Wutzler,[2] L. Rebohle,[2] D. Hiller,[3] J. M. Ramírez,[1] J. A. Rodríguez,[4] W. Skorupa,[2] and B. Garrido[1]
[1]*MIND-IN2UB, Dept. Electrònica, Universitat de Barcelona, Martí i Fanquès 1, 08028 Barcelona, Spain*
[2]*Institute of Ion Beam Physics and Materials Research, Helmholtz-Zentrum Dresden-Rossendorf, P.O. Box 510119, 01314 Dresden, Germany*
[3]*IMTEK, Faculty of Engineering, Albert-Ludwigs-University Freiburg, Georges-Köhler-Allee 103, 79110 Freiburg, Germany*
[4]*Physics Faculty, University of Havana, San Lázaro y L, Vedado, 10400 Havana, Cuba*

(Received 21 June 2013; accepted 26 August 2013; published online 9 September 2013)

High optical power density of 0.5 mW/cm^2, external quantum efficiency of 0.1%, and population inversion of 7% are reported from Tb^+-implanted silicon-rich silicon nitride/oxide light emitting devices. Electrical and electroluminescence mechanisms in these devices were investigated. The excitation cross section for the 543 nm Tb^{3+} emission was estimated under electrical pumping, resulting in a value of 8.2×10^{-14} cm^2, which is one order of magnitude larger than one reported for Tb^{3+}:SiO_2 light emitting devices. These results demonstrate the potentiality of Tb^+-implanted silicon nitride material for the development of integrated light sources compatible with Si technology. © *2013 AIP Publishing LLC*. [http://dx.doi.org/10.1063/1.4820836]

The incorporation of rare earth (RE) ions in a silicon dioxide (SiO_2) matrix sparked the race toward recent routes for developing efficient Si-based light sources compatible with complementary metal-oxide-semiconductor (CMOS) technology. Such light emitters seem an appealing solution to circumvent the microelectronic bottleneck nowadays, for instance, heat dissipation and interconnection problems.[1] Other promising approaches toward this aim are Si-nanocrystals (Si-ncs) embedded in a SiO_2 matrix (SiO_x)[2] and also co-doped with RE ions.[3] Published works run from those covering the visible range with RE ions, such as Ce^{3+},[4] Eu^{3+},[5] and Tb^{3+},[6] to those only focusing on the near infrared region with Nd^{3+} (Ref. 7) and Er^{3+} (Ref. 3) ions. However, little attention has been paid to the electroluminescence (EL) properties of those RE ions embedded either in silicon nitride (Si_3N_4) or silicon-rich silicon nitride (SiN_x) dielectrics. In fact, SiN_x-based materials offer considerable advantages over SiO_x-based active ones: (i) lower carrier injection barrier at the Si/Si_3N_4 interface, giving rise to the fabrication of low-voltage light emitting devices (LEDs),[8] (ii) better electrical stability with direct impact on the device operation lifetimes,[9] and (iii) higher effective refractive index for making high quality resonant cavities.[10] Also, we have recently demonstrated the suitability of SiN_x, in combination with SiO_2 tunnel layers, as promising candidate for the silicon-solid state lighting.[11] Thus, an encouraging scenario toward RE-doped SiN_x LEDs is envisaged. We are only aware of Er-doped SiN_x electroluminescent devices, where the potentiality of this material for the engineering of light emitters at 1.5 μm was reported.[12] Therefore, SiN_x co-doped with RE ions, whose radiative electronic transitions are in the visible range, remains practically unexploited from the electroluminescent viewpoint. Particularly, the most efficient RE ion,[13] namely, Tb^{3+}, is an unexplored candidate embedded in SiN_x for evaluating its electro-optical properties aimed for the realization of integrated, electrically driven Si-based light emitters.

In the present work, the investigation on the nature of electrical and EL mechanisms in Tb^{3+}:SiN_x/SiO_2 LEDs is reported. We demonstrate high optical power density as high as 0.5 mW/cm^2 and we estimate the effective Tb^{3+} excitation cross section as well as the fraction of inverted Tb^{3+} ions. The possibility to obtain integrated Si-based light sources by introducing Tb^{3+} ions in a SiN_x matrix is established.

30 nm-thick SiO_2 and 40 nm-thick SiN_x layers were deposited on highly doped *n*-type Si (100) substrates with resistivity of 1–5 mΩ cm using plasma enhanced chemical vapor deposition (PECVD). An annealing treatment at 1000 °C for 60 min to create the Si-ncs in the silicon nitride layer with 12% of Si excess was performed. The incorporation of Si-ncs was conceived to improve the conductivity and the device operation lifetime.[9] Subsequently, the silicon-rich silicon nitride layer was implanted with Tb^+ ions, whose implantation energy (75 keV) and dose (1.9×10^{15} atoms/cm^2) were adjusted to generate a concentration of nearly 1.5% in the depth range of 20–25 nm. The implantation was followed by post annealing procedure at 900 °C for 30 min in N_2 atmosphere to mitigate defects caused by implantation. On a reference sample, with identical structure and technological parameters but introducing Er^{3+} (a somewhat similar ion in terms of their atomic radii and diffusivity coefficients) instead of Tb^{3+} ions, around 93% of the total ions quantity was determined by secondary ion mass spectroscopy profile into the SiN_x layer. Likewise, no Er^{3+} clusters were detected by energy-filtered transmission electron microscopy images. The preferred gate electrode was a 100 nm transparent indium-tin-oxide (ITO) layer (*n*-type) deposited by rf sputtering. Different circular areas with sizes ranging from 100 μm to 1200 μm diameter were defined by conventional lithography and fabricated. A cross section scheme of the

a)Electronic mail: yberencen@el.ub.edu

obtained devices is shown in Fig. 1(a). Quasi-static current-voltage characteristics (*I-V*) were measured using a semiconductor device analyzer (Agilent B1500A) connected to a probe station (Cascade Microtech Summit 11000) with a Faraday cage. The EL spectra were collected from the top of the devices using a cryogenically cooled Princeton Instruments Spec-10-100B/LN charge-coupled device attached to an Acton 2300i grating spectrometer. Time-resolved EL experiments were conducted using an Agilent 8114A pulse generator, whereas the decay EL traces were recorded with a digital GHz oscilloscope connected to a calibrated photomultiplier (R928). A 1 kΩ resistance in serial connection to back contact of our devices was used for measuring the current passing through it. Both *I-V* and EL measurements were acquired at room temperature by positively biasing the *n*-type ITO electrode, as sketched in Fig. 1(a).

Fig. 1(b) shows the evolution of the current density (J) with the applied voltage (V) ramped at a constant rate of 50 mV/s from 0 V up to just before device breakdown, which occurs at around 41 V. The constant-current density zone of the curve constitutes a measure of the capacitance of the structure $C = J_d S(dV/dt)^{-1}$, which is around 45 pF, where J_d is the displacement current density and S is the electrode area. The *J-V* curve also shows a good concordance with two well-defined conduction mechanisms depending on the voltage values, after the threshold for real current density injection (i.e., for current density typically $>J_d$, $V \sim 21$ V). At moderate voltages, the Poole-Frenkel (PF) mechanism[14] governs the conduction (red solid line), whereas at high voltages the trap-assisted tunneling[15] (TAT) one is predominant

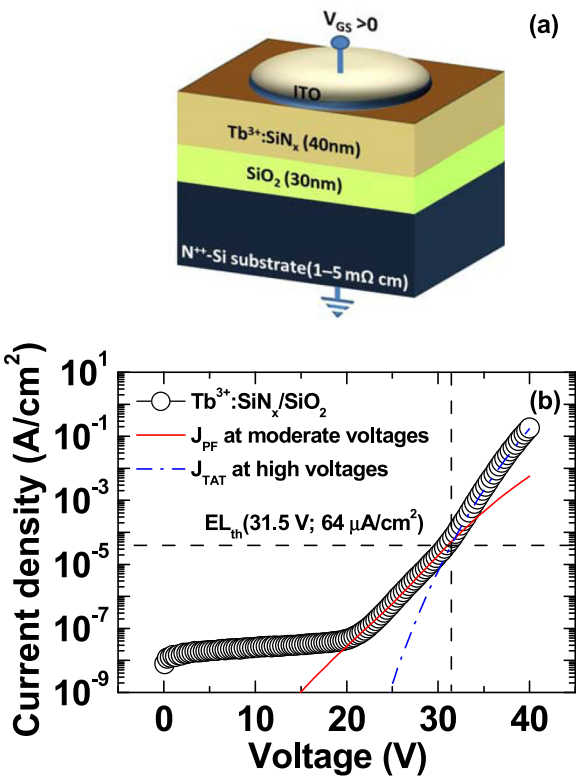

FIG. 1. (a) Cross section scheme of the Tb^{3+}:SiN_x/SiO_2 light emitting device. (b) J-V characteristic of the device showing both fitting models related with Poole-Frenkel and trap-assisted tunneling conduction mechanisms at moderate and high voltages, respectively.

(blue dashed dotted line). Hereafter, we will only pay attention to this latter mechanism because the Tb^{3+} emission takes place solely under this regime, concretely the EL turn on point is at (31.5 V; 64 μA/cm^2) as can be seen in Fig. 1(b). This fact also suggests that the Tb^{3+} excitation is primarily generated by impact ionization by hot electrons in the conduction band, rather than, for instance, by energy transfer from Si-ncs to Tb^{3+} ions.[3] Thus, the electron injection is exclusively limited by the energetic level of the traps situated at the SiO_2 band gap close to the Si/SiO_2 interface. In particular, the trap is energetically placed at around $\Phi_t = (2.0 \pm 0.3)$ eV below the oxide conduction band edge, that is in good agreement with TAT formalism.[15] This value was extracted from the experimental data fitting to the TAT relationship given by $J_{TAT} \propto \exp(-4d_{ox}\sqrt{2m^*}\Phi_t^{3/2}/3q\hbar V_{ox})$, where d_{ox} is the SiO_2 thickness, m^* is the effective electron mass, Φ_t is the trap energy (in eV) below the oxide conduction band edge, q is the electron charge, $\hbar$ is the reduced Planck's constant, and V_{ox} is the voltage drops in the SiO_2 layer. The V_{ox} relationship with the applied voltage (V) is given by $V_{ox} = Vd_{ox}/[d_{ox} + (\varepsilon_{ox}/\varepsilon_{SiN_x})d_{SiN_x}]$, where d_{SiNx} is the SiN_x thickness, as well as $\varepsilon_{ox} = 3.9$ and $\varepsilon_{SiNx} = 7.5$ are the relative permittivity of the SiO_2 and SiN_x, respectively. This conduction mechanism is related to the intrinsic traps created close to the SiO_2/Si-substrate interface due to electric stress generated by effects of high electric field.[15] The introduction of the SiO_2 layer was *ad hoc* conceived for boosting the Tb^{3+} EL by hot electrons. Indeed, this SiO_2 layer introduces a potential energy step of $\sim$1.3 eV at the interface between the SiO_2 and the Si_3N_4 due to the difference in electron affinities (i.e., $SiO_2 = 0.8$ eV and $Si_3N_4 = 2.1$ eV) which offers the possibility of hot electrons injection into the Tb^{3+}:SiN_x active layer. In addition, the SiN_x/SiO_2 bilayer stack was envisaged for achieving a trade-off between EL efficiency and electrical stability of the devices.

Four emission bands in the visible range under direct current pumping were observed. These bands are related to the radiative electronic transitions of Tb^{3+} from $^5D_4$ to $^7F_6$, $^7F_5$, $^7F_4$, and $^7F_3$ energetic states,[13] respectively, as shown in Fig. 2(a). The line-shape of the measured spectra for different constant current values does also not change (i.e., the emission lines preserve their relative intensities). Moreover, a broad EL band peaking at 465 nm from non-implanted Tb^+ reference device was detected. In former published works, this emission was ascribed to Si-related defects in silicon nitride.[16] However, this electroluminescence was not clearly observed in the studied devices due to the overlapping with the intense Tb^{3+} emission. Fig. 2(b) depicts a linear dependence of the optical power density with respect to the injected current density. An optical power density as high as 0.5 mW/cm^2 is reached at the highest current density, where a light saturation is clearly observed on the graph. This is the largest optical power density value ever reported for Tb^+-implanted SiN_x LEDs. Moreover, an external quantum efficiency (EQE) of 0.1% is obtained. This EQE value is also the highest ever reported for RE in SiN_x matrices, that is comparable with the one obtained for Er^{3+}:SRO LEDs.[17] Strong green-yellow emission coming from the top of the devices is observed to naked eye under daylight conditions as well as very stable over hours. This green-yellow light is

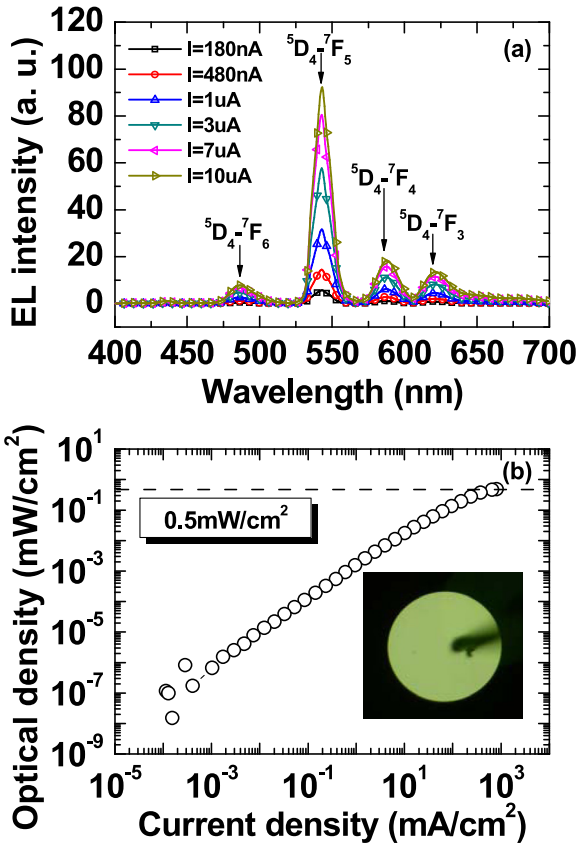

FIG. 2. (a) Electroluminescence spectra at different constant current values and several Tb^{3+} electronic transitions from $^5D_4$ to $^7F_6$, $^7F_5$, $^7F_4$, and $^7F_3$, respectively. (b) Optical power density versus current density. Inset shows green-yellow emission at naked eyes.

ascribed to the main Tb^{3+} radiative electronic transition ($^5D_4$-$^7F_5$) at 543 nm, which is responsible of the 58% of the overall emission in our devices. In the inset of Fig. 2(b), a photograph collected from the emission area of the device by a commercial digital camera demonstrates this latter fact. This emission line is also close to the wavelength of 555 nm, where the human eye sensitivity is maximal.[18] Therefore, taking advantage of the high optical power density at the most suitable wavelength, an encouraging scenario can be envisaged for the development of silicon-based solid state lighting. A detailed photometric study, including color quality, color rendering, and luminous efficacy of radiation, is currently in progress in this materials platform.

Under alternate current pumping, the electrical excitation cross section (σ) of the Tb^{3+} at 543 nm was calculated by measuring the EL rise time (τ_{rise}) at different excitation square pulses. Fig. 3 shows that the EL decay time (τ_{decay}) remains constant with respect to the charge flux (ϕ), whereas the EL rise time drops as the charge flux increases. This behavior is consistent with a two-level system at low fluxes, where σ does not depend of the injected electron flux.[19] Hence, using the expression $1/\tau_{rise} = \sigma\phi + 1/\tau_{decay}$, we can deduce the electrical cross section of the Tb^{3+} 543 nm emission by a linear fit.[12] Prior to that, both EL rise and decay times were well-fitted by a single exponential function. The EL rise time values at different charge fluxes range from 0.5 ms to 0.7 ms, whereas the EL decay time was found to be 0.5 ms, which is close to the one measured under optical

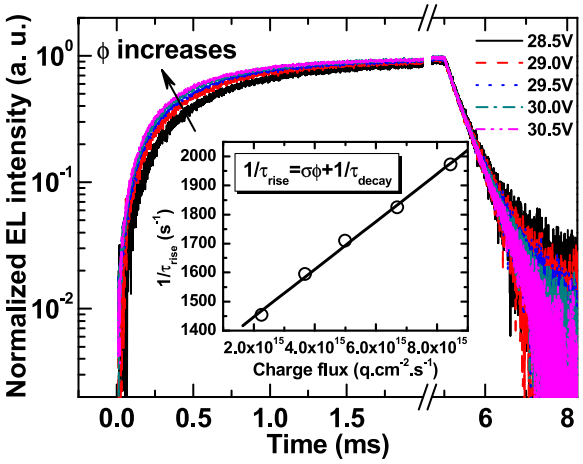

FIG. 3. Normalized EL intensity as a function of time excited by different square voltage pulses. Inset: Linear relationship of the inverse rise time ($1/\tau_{rise}$) of the EL at 543 nm with respect to charge flux (ϕ) considering a two-level system at low flux regime.

pumping in Tb^{3+}:SiO_2 films.[20] The inset of Fig. 3 depicts the linear relationship between the inverse rise time and charge flux. The charge flux was calculated taking into account the measured current through 1 kΩ resistance in serial connection to back contact of our devices instead of using the injected current deduced from the applied voltage. Therefore, the Tb^{3+} excitation cross section at 543 nm was found to be $(8.2 \pm 0.5) \times 10^{-14}$ cm^2, that is one order of magnitude larger than one reported for Tb^+-implanted SiO_2 light emitting devices under electrical pumping.[6] As a consequence, the probability of Tb^{3+} excitation in silicon nitride is higher than the silicon dioxide matrix.

In order to estimate the fraction of inverted Tb^{3+} ions (N_2) in the main radiative electronic transition ($^5D_4$-$^7F_5$) at 543 nm, we used the following formula:[17] $N_2 = D_{opt} \cdot \tau_{rad}/\hbar\varpi \cdot d$, where D_{opt} is the emitted optical power density, τ_{rad} is the Tb^{3+} radiative lifetime, and $\hbar\varpi$ is the photon energy. Therefore, the maximum emitted optical power density can be calculated considering the following circumstances: (i) the number of introduced Tb^{3+} ions is 4.8×10^{20} at/cm^3, which corresponds to a maximum power density value of 4.8×10^{20} photons/cm^3 and (ii) a Tb^{3+} radiative lifetime of 3.5 ms. This Tb^{3+} radiative lifetime value was chosen taking into account that had been reported for two different host matrices,[21,22] which suggests to be not strongly sensitive to the matrix-type. Taking the measured EL decay time value of 0.5 ms would neglect all Tb^{3+} ions that are excited, but will relax in a non-radiative way. Then, the total internal emitted power density is 0.2 W/cm^2. However, the fraction of emitted light able to escape from electrode and collected by our microscope objective with 0.4 of numerical aperture was found to be 4%. The collection angle (23.5°) related with the numerical aperture of the used microscope objective is lesser than the critical angle (30°) associated to the total internal reflection phenomena inside the active layer. Additionally, 91% of the emitted light is transmitted at 543 nm through the 100 nm ITO electrode. Therefore, the out-coupling efficiency is around 3.6%. Hence, taking into account these corrections the external optical power density is 7.2 mW/cm^2. Now, comparing this latter value with the

maximum measured optical power density (0.5 mW/cm^2) from our device, we get an optical power density ratio of about 7%, which corresponds to the fraction of inverted Tb^{3+} ions at steady state. This value is still far from 50% that is the minimum required to achieve lasing action. The precedent calculation had not been reported before for Tb^+-implanted SiN_x/SiO_2 light emitting devices, even though the results are still lower than those previously published for Er^{3+}:SRO-based devices, where 20% of inverted Er^{3+} ions was reported.[17]

In conclusion, Tb^+-implanted SiN_x/SiO_2 light emitting devices with optical power density as high as 0.5 mW/cm^2 and EQE of 0.1% were fabricated. The EL mechanism of the devices can be ascribed to impact ionization of the Tb^{3+} luminescent centers by hot electrons with cross section of 8.2×10^{-14} cm^2. A Tb^{3+} population inversion of 7% under electrical pumping was estimated. The suitability of this materials platform for the realization of integrated Si-based light emitters fully compatible with CMOS technology was demonstrated.

This work was financially supported by the Spanish Ministry of Science and Innovation (Project No. TEC2009-08359). Y.B. acknowledges the financial support from Grant No. EEBB-I-2012-04552 during his research stay at *Helmholtz-Zentrum Dresden-Rossendorf* in Germany. The authors also thank the Rossendorf implantation and clean room facility group for ion implantation and clean room preparations, respectively.

[1]L. C. Kimerling, L. Dal Negro, S. Saini, Y. Yi, D. Ahn, S. Akiyama, D. Cannon, J. Liu, J. G. Sandland, D. Sparacin, J. Michel, K. Wada, and M. R. Watts, in *Silicon Photonics*, edited by L. Pavesi and D. J. Lockwood (Springer, New York, 2004).
[2]C.-H. Cheng, Y.-C. Lien, C.-L. Wu, and G.-R. Lin, Opt. Express **21**, 391 (2013).
[3]J. M. Ramírez, F. Ferrarese Lupi, O. Jambois, Y. Berencén, D. Navarro-Urrios, A. Anopchenko, A. Marconi, N. Prtljaga, A. Tengattini, L. Pavesi, J. P. Colonna, J. M. Fedeli, and B. Garrido, Nanotechnology **23**, 125203 (2012).
[4]J. M. Sun, S. Prucnal, W. Skorupa, M. Helm, L. Rebohle, and T. Gebel, Appl. Phys. Lett. **89**, 091908 (2006).
[5]S. Prucnal, J. M. Sun, W. Skorupa, and M. Helm, Appl. Phys. Lett. **90**, 181121 (2007).
[6]J. M. Sun, W. Skorupa, T. Dekorsy, M. Helm, L. Rebohle, and T. Gebel, J. Appl. Phys. **97**, 123513 (2005).
[7]O. Debieu, J. Cardin, X. Portier, and F. Gourbilleau, Nanoscale Res. Lett. **6**, 161 (2011).
[8]R. Huang, K. Chen, H. Dong, D. Wang, H. Dong, W. Li, J. Xu, Z. Ma, and L. Xu, Appl. Phys. Lett. **91**, 111104 (2007).
[9]Y. Berencén, J. M. Ramírez, and B. Garrido, in Proceedings of the 2013 Spanish Conference on Electron Devices, CDE 2013, (IEEE Xplore, Valladolid, 2013).
[10]M. Makarova, V. Sih, J. Warga, R. Li, L. Dal Negro, and J. Vuckovic, Appl. Phys. Lett. **92**, 161107 (2008).
[11]Y. Berencén, J. Carreras, O. Jambois, J. M. Ramírez, J. A. Rodríguez, C. Domínguez, C. E. Hunt, and B. Garrido, Opt. Express **19**, A234 (2011).
[12]S. Yerci, R. Li, and L. Dal Negro, Appl. Phys. Lett. **97**, 081109 (2010).
[13]L. Rebohle and W. Skorupa, *Rare-Earth Implanted MOS Devices for Silicon Photonics* (Springer, Heidelberg, 2010).
[14]O. Jambois, Y. Berencén, K. Hijazi, M. Wojdak, A. J. Kenyon, F. Gourbilleau, R. Rizk, and B. Garrido, J. Appl. Phys. **106**, 063526 (2009).
[15]M. P. Houng, Y. H. Wang, and W. J. Chang, J. Appl. Phys. **86**, 1488 (1999).
[16]Z. H. Cen, T. P. Chen, L. Ding, Y. Liu, J. I. Wong, M. Yang, Z. Liu, W. P. Goh, F. R. Zhu, and S. Fung, Appl. Phys. Lett. **94**, 041102 (2009).
[17]O. Jambois, F. Gourbilleau, A. J. Kenyon, J. Montserrat, R. Rizk, and B. Garrido, Opt. Express **18**, 2230 (2010).
[18]E. Fred Schubert, *Light Emitting Diodes*, 2nd ed. (Cambridge University Press, New York, 2006).
[19]S. Wang, A. Eckau, E. Neufeld, R. Carius, and Ch. Buchal, Appl. Phys. Lett. **71**, 2824 (1997).
[20]A. Podhorodecki, G. Zatryb, J. Misiewicz, J. Wojcik, P. R. J. Wilson, and P. Mascher, Nanotechnology **23**, 475707 (2012).
[21]D. K. Sardar, K. L. Nash, R. M. Yow, J. B. Gruber, U. V. Valiev, and E. P. Kokanyan, J. Appl. Phys. **100**, 083108 (2006).
[22]W. Di, X. Wang, B. Chen, S. Lu, and X. Zhao, J. Phys. Chem. B **109**, 13154 (2005).